Bacterial immunotherapy for cancer induces CD4-dependent tumor-specific immunity through tumor-intrinsic interferon-γ signaling

Anthony C. Antonelli[a,b], Anna Binyamin[b], Tobias M. Hohl[a,b,c], Michael S. Glickman[a,b,c,1], and Gil Redelman-Sidi[c,1]

[a]Immunology and Microbial Pathogenesis, Weill Cornell Medicine Graduate School of Medical Sciences, New York, NY 10065; [b]Immunology Program, Sloan Kettering Institute, Memorial Sloan Kettering Cancer Center, New York, NY 10065; and [c]Division of Infectious Diseases, Memorial Sloan Kettering Cancer Center, New York, NY 10021

Bacillus Calmette–Guérin (BCG) immunotherapy for bladder cancer is the only bacterial cancer therapy approved for clinical use. Although presumed to induce T cell-mediated immunity, whether tumor elimination depends on bacteria-specific or tumor-specific immunity is unknown. Herein we show that BCG-induced bladder tumor elimination requires CD4 and CD8 T cells, although augmentation or inhibition of bacterial antigen-specific T cell responses does not alter the efficacy of BCG-induced tumor elimination. In contrast, BCG stimulates long-term tumor-specific immunity that primarily depends on CD4 T cells. We demonstrate that BCG therapy results in enhanced effector function of tumor-specific CD4 T cells, mainly through enhanced production of IFN-γ. Accordingly, BCG-induced tumor elimination and tumor-specific immune memory require tumor cell expression of the IFN-γ receptor, but not MHC class II. Our findings establish that a bacterial immunotherapy for cancer is capable of inducing tumor immunity, an antitumor effect that results from enhanced function of tumor-specific CD4 T cells, and ultimately requires tumor-intrinsic IFN-γ signaling, via a mechanism that is distinct from other tumor immunotherapies.

BCG | T cell | immunotherapy | tumor immunity | bladder cancer

The use of bacteria as a cancer immunotherapy was pioneered in the late 19th century with the work of William B. Coley. Following observations of tumor regression coincident with bacterial infections, Coley began conducting experiments with intratumoral injections of live cultures of *Streptococcus pyogenes*, and subsequently lysates derived from cultures of *S. pyogenes* and *Serratia marcescens*. These so-called Coley's toxins were used in the United States to treat tumors from 1893 to 1963. However, they had mixed clinical success and their mechanism of action was never determined (1, 2).

Bacillus Calmette–Guérin (BCG) is an attenuated strain of *Mycobacterium bovis* originally developed as a vaccine against tuberculosis. Early data demonstrated that mice infected intravenously with BCG were more resistant to transplantation of tumors (3). Subsequently, BCG immunotherapy was used for various cancers, including leukemia and melanoma (4, 5), followed in 1976 by the first report of a successful use of BCG to treat patients with bladder cancer (6).

While no longer in use for other cancers, BCG remains the standard of care for many patients with nonmuscle-invasive bladder cancer (NMIBC). In these patients, BCG decreases the risk of cancer recurrence (7, 8) and reduces the risk of progression to invasive disease (9). Relative to other microbial treatments for cancer, which remain largely experimental (10), such as oncolytic viruses, BCG therapy is arguably not only the most successful microbial therapy for cancer in current clinical use, but one of the more successful immunotherapies for cancer in general, highlighting the therapeutic potential of a more complete understanding of the relationship between the immune system, infection, and cancer. To date, BCG remains the only bacterial

cancer immunotherapy established as a standard of care since becoming the first ever immunotherapy approved by the Food and Drug Administration in 1990. Despite its remarkable success, the mechanism by which BCG induces a tumor-eliminating immune response is still unclear (11).

Prior studies have suggested that T cells are required for BCG therapy (12), although there remains controversy over whether the antigenic targets of these T cells are of mycobacterial or tumor origin (13). To this end, Biot et al. (14) showed that BCG therapy results in expansion of BCG-specific T cells in the bladder-draining lymph nodes (LNs), and that subcutaneous immunization with BCG prior to tumor implantation and treatment results in improved tumor elimination by BCG. Biot et al. also found a correlation between tuberculin skin test positivity at baseline and improved recurrence-free survival in patients with NMIBC who received BCG, although these findings have not been universally replicated (15, 16). Based on these results, Biot et al. (14) concluded that activation of BCG-specific T cells is required for the efficacy of BCG. These conclusions have set the current direction of study in the field, whereby strategies to enhance BCG-specific T cell immunity are currently being studied in patients receiving BCG for NMIBC (17, 18).

In contrast to the current paradigm for BCG therapy, the efficacy of other tumor immunotherapies, such as immune checkpoint blockade therapy, appears to rely on the activation of tumor-specific T cells, particularly within the CD8 T cell compartment (19–22). Consistent with these data, T cells reactive

---

Significance

Bacillus Calmette–Guérin (BCG) therapy is one of the oldest tumor immunotherapies, but its mechanism remains unknown. Herein we show that BCG therapy induces tumor-specific T cell-dependent immunity that is predominantly mediated by CD4 T cells in a manner distinct from other tumor immunotherapies. These immunologic insights may allow investigation into biomarkers that could predict the efficacy of BCG in human cancer patients.

against tumor neoantigens were recently identified in a patient with NMIBC who had previously received BCG (23), suggesting that tumor-specific T cells could also play a role in the context of BCG therapy.

Herein, we utilize a BCG-responsive orthotopic model of bladder cancer to dissect the immunologic mechanism of BCG-induced tumor elimination and demonstrate that BCG induces a tumor-specific immune response that is dependent on tumor-specific CD4 T cells. We show that BCG therapy results in enhanced effector functions of tumor-specific CD4 T cells, and furthermore acts through the IFN-γ receptor (IFNGR) on tumor cells. In contrast, we find no role for bacteria-specific T cells in the antitumor effect of BCG.

Results

To investigate the immune mechanisms of BCG-induced tumor elimination, we used the murine MB49 orthotopic model of bladder cancer (*SI Appendix*, Fig. S1*A*). In this model, mice are implanted with the syngeneic MB49 tumor cell line, and weekly intravesical treatments of 3×10^6 colony-forming units (CFU) of BCG result in 20 to 50% long-term survival as compared to only 0 to 10% survival in PBS-treated mice (*SI Appendix*, Fig. S1*B*).

BCG Treatment for Bladder Tumors Results in Activation of Tumor-Infiltrating T Cells. To characterize tumor-infiltrating lymphocytes in BCG-treated mice as compared to PBS-treated controls, we performed flow cytometric analysis of MB49 bladder tumors from mice that received three weekly intravesical treatments of BCG or PBS (Fig. 1*A* and *SI Appendix*, Fig. S1*C*). We found no significant differences between BCG- and PBS-treated mice in overall abundance of total lymphocytes (CD45$^+$), NK cells (NK1.1$^+$), or B cells (CD19$^+$) (Fig. 1 *B–D*). There was, however, a higher proportion of CD4 T cells in the bladders of BCG-treated mice (Fig. 1*E*), a finding consistent with

observations from a rat orthotopic model of BCG (24). Among BCG-treated mice, CD4 T cells showed evidence of increased proliferation and differentiation, as measured by Ki67, CD44, and CD62L expression, as well as decreased expression of the hallmark exhaustion markers programmed cell death protein 1 (PD-1) and lymphocyte-activation gene 3 (LAG-3) compared to PBS-treated mice (Fig. 1 *F–H*). There was no significant difference in the abundance of CD8 T cells between BCG- and PBS-treated mice (Fig. 1*I*), although there was higher proliferation among CD8 T cells in the BCG-treated mice (Fig. 1*J*). Additional phenotypic comparisons between BCG- and PBS-treated mice are shown in *SI Appendix*, Fig. S2.

These data demonstrate that treatment of bladder tumors with BCG results in increased proliferation and differentiation, and decreased exhaustion of tumor-infiltrating CD4 and, to a lesser extent CD8 T cells.

BCG-Induced Bladder Tumor Elimination Requires CD4 and CD8 T Cells. A seminal study in the field of BCG therapy for bladder cancer suggested that CD4 and CD8 T cells are both required for the efficacy of BCG (12), although these conclusions were based on the effect of T cell depletion on tumor size as estimated by abdominal palpation, rather than on overall mouse survival or measures of tumor immunity. We sought to definitively determine the effect of CD4 and CD8 T cell depletion on mouse survival in the MB49 orthotopic model. Mice were treated with CD4- or CD8-depleting antibodies, followed by implantation of MB49 bladder tumors and weekly intravesical instillations of BCG or PBS (Fig. 2*A*). Robust depletion of CD4 and CD8 T cells was confirmed on day 7 following tumor implantation, by flow cytometric analysis of peripheral blood mononuclear cells (PBMCs) (Fig. 2 *B* and *C*), and antibody administration was maintained throughout the course of the study. Tumor uptake was also measured by bioluminescence imaging of tumor cell luciferase
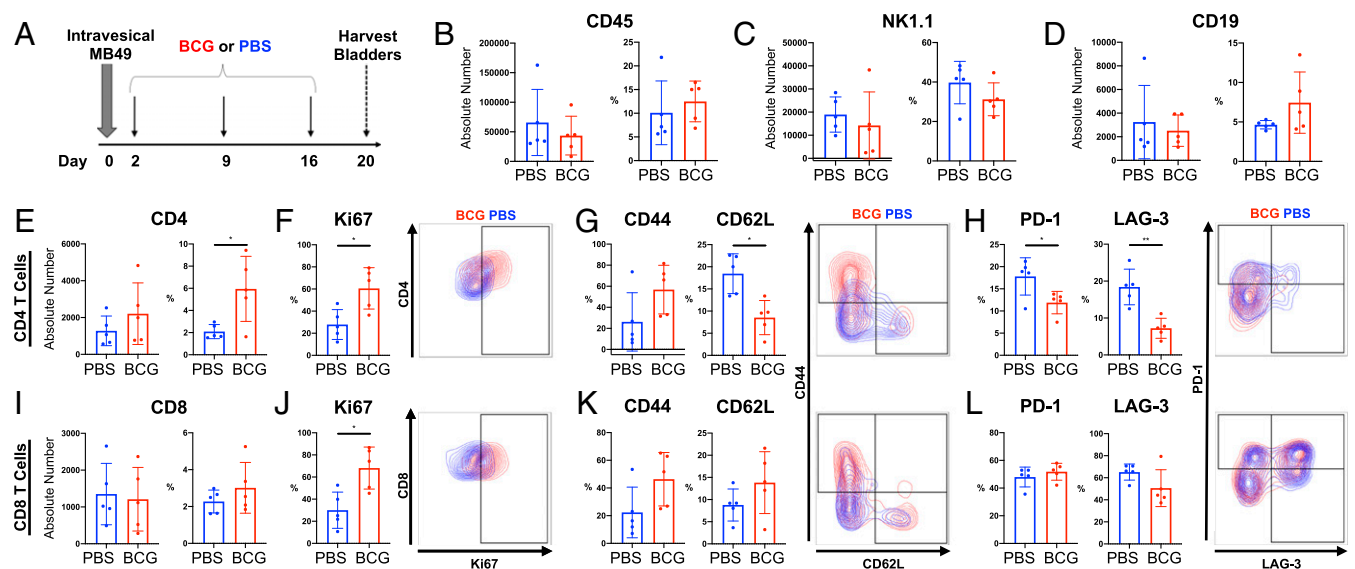

Fig. 1. BCG treatment for bladder tumors results in activation of tumor-infiltrating T cells. (*A*) Experimental schematic. Mice were implanted with MB49 bladder tumors on day 0 and received intravesical BCG or PBS on days 2, 9, and 16. On day 20 the mice were killed, and tumor single-cell suspensions were stained and evaluated by flow cytometry. Absolute number refers to the number of cells in the entirety of each sample. (*B–L*) Comparison of BCG- versus PBS-treated bladders for (*B*) CD45$^+$ absolute numbers and percent of total live cells, (*C*) NK1.1$^+$ absolute numbers and percent of CD45$^+$ live cells, (*D*) CD19$^+$ absolute numbers and percent of CD45$^+$ live cells, and (*E*) CD4$^+$FOXP3$^-$ T cell absolute numbers and percent of live CD45$^+$ cells. (*F*) Percent Ki67$^+$ of CD4$^+$FOXP3$^-$ T cells. Representative flow plot is shown. (*G*) Percent CD44$^+$ and CD62L$^+$ of CD4$^+$FOXP3$^-$ T cells. Representative flow plot is shown. (*H*) Percent PD1$^+$ and LAG-3$^+$ of CD4$^+$FOXP3$^-$ T cells. Representative flow plot is shown. (*I*) CD8$^+$ T cell absolute numbers and percent of live CD45$^+$ cells. (*J*) Percent Ki67$^+$ of CD8$^+$ T cells. Representative flow plot is shown. (*K*) Percent CD44$^+$ and CD62L$^+$ of CD8$^+$ T cells. Representative flow plot is shown. (*L*) Percent PD1$^+$ and LAG-3$^+$ of CD8$^+$ T cells. Representative flow plot is shown. Data are representative of two independent experiments. Error bars represent average ± SD. *P* values were derived by Student's *t* test. See also *SI Appendix*, Fig. S2. *$P < 0.05$; **$P < 0.005$.
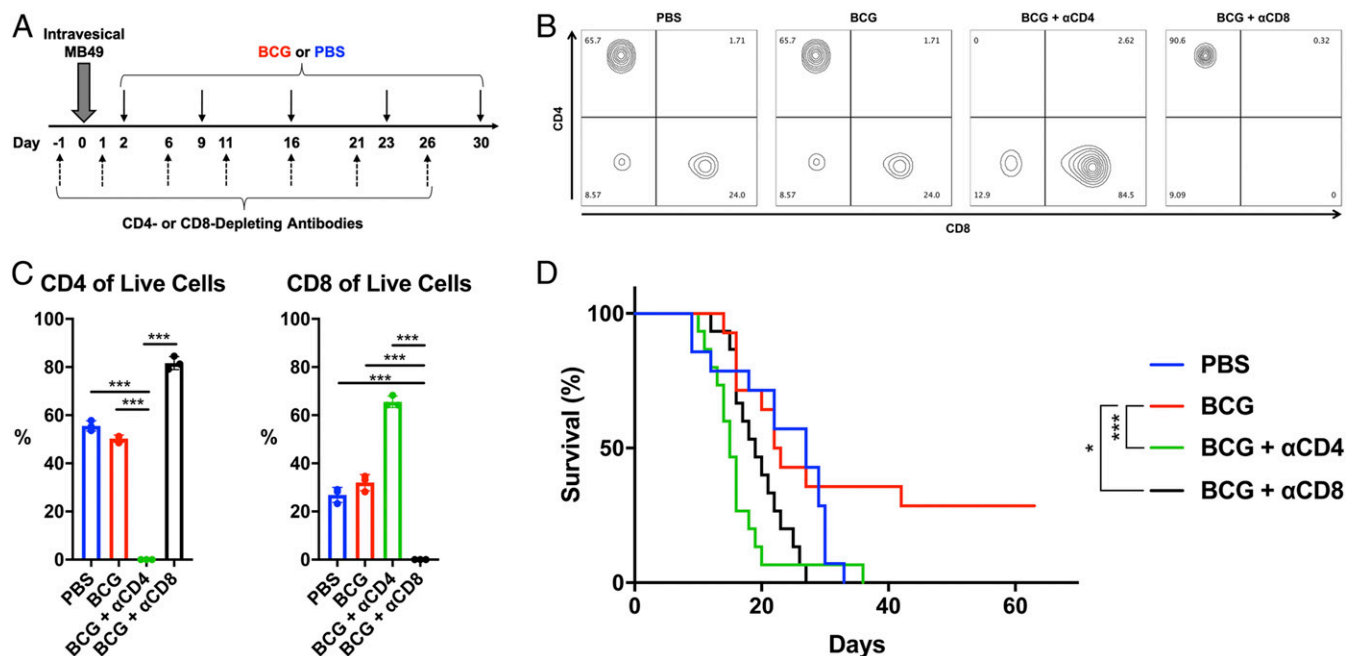
www.manaraa.com

Fig. 2. BCG-induced tumor elimination requires CD4 and CD8 T cells. (*A*) Experimental schematic for T cell depletion using anti-CD4 (αCD4) or anti-CD8 (αCD8) antibodies in mice with MB49 tumors receiving intravesical BCG or PBS. (*B*) On day 7 of the experiment shown in *A*, blood was collected from three mice in each group and T cell depletion was assessed by flow cytometry (representative plots shown). (*C*) Percent CD4 and CD8 T cells of PBMCs for $n = 3$ mice per group. Error bars represent average ± SD. *P* values were derived by one-way ANOVA with Bonferroni's multiple comparisons test. (*D*) Survival of CD4- and CD8-depleted mice. *P* values derived by log-rank test. See also *SI Appendix*, Fig. S3. *$P < 0.05$; ***$P < 0.0005$.

activity on day 7 postimplantation and showed no difference in tumor establishment between groups (*SI Appendix*, Fig. S3*A*). Depletion of either CD4 or CD8 T cells resulted in complete abrogation of the efficacy of BCG (Fig. 2*D*). Notably, BCG-treated animals depleted of CD4 or CD8 T cells succumbed to tumors even more rapidly than immunocompetent untreated animals. Although there are several potential explanations for this observation, including increased BCG toxicity or alternative myeloid phenotypes in the absence of T cells, one compelling hypothesis that requires further investigation is that immunosurveillance by tumor-specific T cells is occurring even in the absence of BCG therapy, albeit functionally insufficient to eliminate the tumor. These results nevertheless confirm the requirement of both CD4 and CD8 T cells for tumor elimination by BCG.

Augmentation of BCG-Specific T Cell Responses Does Not Improve the Efficacy of BCG Therapy. The data above demonstrate that BCG results in activation of T cells, and that both CD4 and CD8 T cells are required for BCG efficacy; however, the antigenic specificity at the heart of this T cell requirement—be it BCG-specific, tumor-specific, or both—remains undetermined.

It has been suggested that the efficacy of BCG therapy depends on BCG transport to the bladder-draining LNs, BCG-specific T cell priming, and migration of BCG-specific T cells to the bladder (14). In *Mycobacterium tuberculosis* lung infection, CCR2$^+$ inflammatory monocytes are required for mycobacterial transport to the mediastinal LNs and T cell priming (25). We hypothesized that this mechanism might be operative in BCG transport to the bladder-draining LNs, and might provide a mechanism to test the role of BCG-specific T cell priming in the antitumor response. It was previously shown that BCG cannot be isolated from bladders 24 h after intravesical treatment, but could be found in the bladder-draining LNs (14). We thus determined the temporal dynamics of BCG transport to the bladder-draining LNs. We found that in mice treated with weekly

intravesical BCG instillations, BCG was detected in the bladder-draining LNs as early as 1 wk after initial administration, and BCG LN titers peaked at 2 wk (Fig. 3*A*), consistent with the kinetics of BCG-specific T cell priming. To test whether inflammatory monocytes are also required for BCG transport from the bladder to the bladder-draining LNs, we used CCR2-DTR mice, in which administration of diphtheria toxin (DT) results in specific depletion of CCR2$^+$ cells, including inflammatory monocytes (*SI Appendix*, Fig. S4*A*). We found that depletion of CCR2$^+$ cells resulted in a nearly 10-fold reduction in BCG bacterial load in the bladder-draining LNs, confirming a role for these cells in the transport of BCG from the bladder to the bladder-draining LNs (Fig. 3*B*). However, despite abrogation of BCG transport to the bladder-draining LNs, BCG maintained its antitumor effect (Fig. 3*C*).

Prior data indicated that subcutaneous immunization with BCG before implantation of MB49 tumors dramatically improved the survival of tumor-bearing mice treated with intravesical BCG (14). Using the same treatment schedule (*SI Appendix*, Fig. S4*B*), we demonstrated a similar trend, although the survival benefit conferred by subcutaneous BCG in our hands was not as substantial (*SI Appendix*, Fig. S4*C*).

To investigate whether boosting BCG-specific T cell immunity improves the efficacy of BCG, we employed CD4 T cells from P25 transgenic mice, which bear T cell receptors (TCRs) specific to Ag85b, a mycobacterial antigen expressed by BCG (26). Most CD4 T cells from P25 mice have a naive phenotype at baseline (*SI Appendix*, Fig. S4*D*). To determine whether intravesical BCG results in activation of BCG-specific T cells, we transferred 1 million congenically marked CD45.1$^+$ P25 CD4 T cells into MB49 tumor-bearing mice receiving intravesical BCG or PBS (Fig. 3*D*). Thirteen days after bladder tumor implantation, we removed the bladder-draining LNs and assessed the presence and activation of the transferred BCG-specific CD4 T cells. BCG treatment resulted in recruitment of P25 CD4 T cells to the
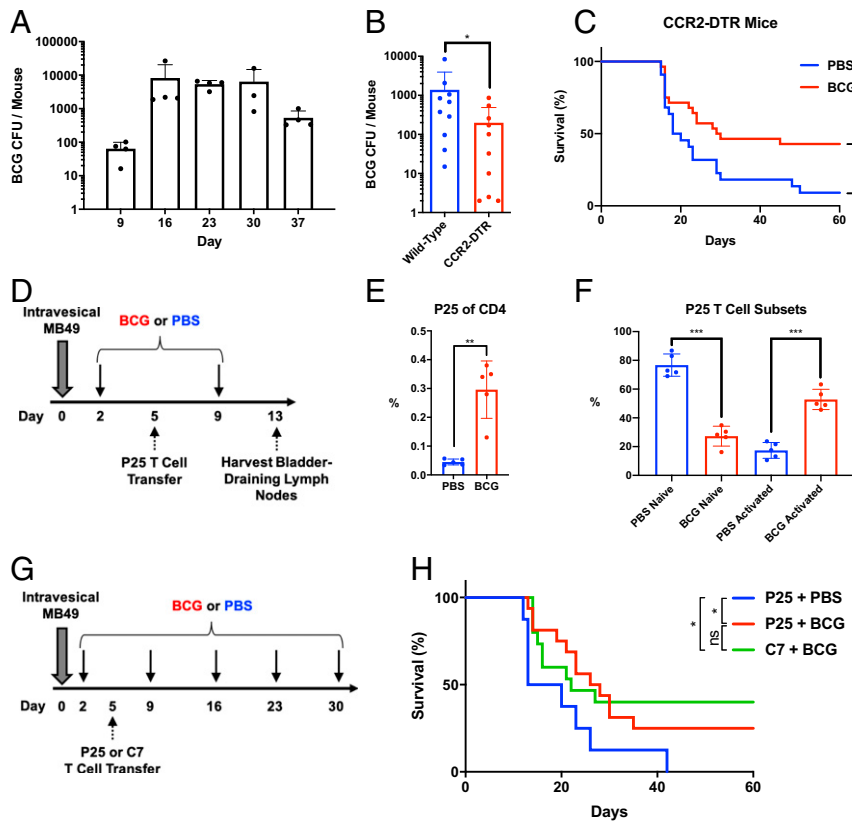
Antonelli et al.

Fig. 3. BCG-directed T cell immunity is not required for BCG-induced tumor clearance. (*A*) Mice were implanted with MB49 bladder tumors on day 0 and received intravesical BCG on days 2, 9, 16, 23, and 30. On days 9, 16, 23, 30, and 37, bladder-draining LNs were removed from four of the mice and homogenates cultured to determine the number of BCG CFU. Data are representative of two independent experiments. Error bars represent mean ± SD. (*B*) Wild-type and CCR2-DTR mice were implanted with MB49 bladder tumors on day 0 and received intravesical BCG or PBS on days 2 and 9. Intraperitoneal DT was injected 4 h before and 48 h after each BCG or PBS treatment. On day 14, bladder-draining LNs were removed, and cell lysates were plated on mycobacterial growth plates to determine the number of BCG CFU. Data represent two independent experiments. Error bars represent mean ± SD. *P* value derived by Student's *t* test. (*C*) Survival of CCR2-DTR mice. CCR2-DTR mice were implanted with MB49 bladder tumors on day 0 and received intravesical BCG or PBS on days 2, 9, 16, 23, and 30. Intraperitoneal DT was injected 4 h before and 48 h after BCG or PBS administration on days 2 and 9. Data represent two independent experiments. *P* value derived by log-rank test. (*D*) Experimental schematic. Mice were implanted with MB49 bladder tumors on day 0 and received intravesical BCG or PBS on days 2 and 9. On day 5, 1×10^6 P25 CD4$^+$CD45.1$^+$CD45.2$^+$ T cells were transferred via retro-orbital injection. On day 13, bladder-draining LNs were removed and analyzed by flow cytometry. (*E*) Proportion of CD45.1$^+$ cells of CD3$^+$CD4$^+$ cells in the bladder-draining LNs of BCG- versus PBS-treated mice. *P* value derived by Student's *t* test. (*F*) Proportions of naive (CD62L$^+$CD44$^-$) and activated (CD44$^+$) of CD45.1$^+$CD4$^+$ cells in the bladder-draining LNs of BCG- versus PBS-treated mice. Error bars represent average ± SD. *P* values derived by Student's *t* test. (*G*) Experimental schematic. Mice were implanted with MB49 bladder tumors on day 0 and received intravesical BCG or PBS on days 2, 9, 16, 23, and 30. On day 5, mice received 1×10^6 CD4 T cells from P25 or C7 mice via retro-orbital injection. (*H*) Survival curves of mice from *G*. *P* values derived by log-rank test. See also *SI Appendix*, Fig. S4. *$P < 0.05$; **$P < 0.005$; ***$P < 0.0005$; ns, nonsignificant.

bladder-draining LNs (Fig. 3*E*), and these CD4 T cells were activated, as determined by a lower proportion of naive T cell subsets, and a higher proportion of effector/effector memory and central memory T cell subsets in the BCG-treated mice (Fig. 3*F*). These results confirm prior findings that intravesical BCG activates a BCG-specific T cell response.

To determine whether enhancement of BCG-specific T cell immunity could augment the efficacy of BCG, we transferred P25 CD4 T cells to mice receiving BCG or PBS for MB49 tumors and monitored survival. As a control, we transferred CD4 T cells from C7 transgenic mice, which express a TCR specific for ESAT-6, a major antigenic determinant of the immune response to *M. tuberculosis* that is genetically absent from BCG (27) (Fig. 3*G*). We observed that BCG-treated mice that received P25 CD4 T cells did not have any survival advantage compared to BCG-treated mice that received antigenically irrelevant C7 CD4 T cells (Fig. 3*H*). Although Ag85b is a well-documented antigenic determinant of the response to BCG vaccination, it is conceivable that T cell responses to Ag85b are not important for the efficacy of BCG therapy for bladder cancer, that greater

numbers of P25 T cells are required than those that resulted from our adoptive transfer, or that a broader T cell response to numerous BCG antigens is required in order to boost BCG efficacy in the context of bladder cancer. While our results, therefore, do not rule out a role for BCG-specific T cells in the mechanism of BCG, they also do not support a model in which BCG antigen-specific T cell responses determine the antitumor effect of BCG.

BCG Induces T Cell-Dependent Tumor-Specific Immunity. Having established that BCG-specific T cells are not sufficient for tumor elimination, we next explored the possibility that BCG provokes a tumor-specific T cell response. Induction of a tumor-specific T cell response by BCG would be expected to result in tumor-specific immunity. To test this hypothesis, we generated a cohort of mice cured of MB49 bladder tumors by BCG (survivor mice) and attempted to reimplant MB49 bladder tumors. We found that these mice were completely resistant to reimplantation of MB49 tumors in their bladders (Fig. 4*A*). However, we reasoned that resistance to tumor reimplantation in the bladder could also

be driven by nonspecific local inflammatory changes induced by prior intravesical BCG treatments. To test whether successful BCG therapy of MB49 bladder tumors results in true systemic immunity to MB49 tumors, we generated an additional cohort of mice cured of MB49 bladder tumors by BCG, as well as control groups treated with intravesical BCG alone (in the absence of MB49 bladder tumors) or naive mice that received neither intravesical MB49 nor intravesical BCG. Six weeks after the last BCG treatment, all groups of mice were challenged with subcutaneous MB49 flank tumors and monitored for tumor growth (Fig. 4B). We observed that mice cured of MB49 by BCG, but not mice who received BCG alone, rejected MB49 tumors upon rechallenge (Fig. 4C).

To test whether the tumor immunity engendered by BCG is specific to MB49 tumors, we repeated the rechallenge experiment described in Fig. 4B with MB49 tumors in one flank but introduced antigenically distinct B16 melanoma tumors in the opposite flank. We found that mice successfully cured of MB49 bladder tumors by BCG were resistant to rechallenge with MB49 tumors but not to B16 tumors (Fig. 4D), demonstrating that the immunity induced by BCG is tumor-specific.

The data presented above suggest that BCG-induced tumor elimination depends on both CD4 and CD8 T cells, and that this tumor elimination results in durable tumor-specific immunity. To determine the role of CD4 and CD8 T cells in BCG-induced tumor-specific immunity, we depleted CD4 or CD8 T cells prior to rechallenging BCG-cured mice with subcutaneous MB49 flank tumors (Fig. 4E and *SI Appendix*, Fig. S3B). We found that CD4 depletion resulted in near-complete abrogation of tumor-specific immunity, whereas CD8 depletion had a subtler effect, maintaining partial control of tumor growth, although not to the same degree as fully immunocompetent survivor mice (Fig. 4F).

To determine whether transfer of tumor-specific T cells could improve control of MB49 bladder tumors in naive mice, we isolated T cells from mice cured of MB49 tumors by BCG (MB49+BCG), mice that received BCG treatment in the absence of MB49 bladder tumors (BCG only), or from untreated, nontumor-bearing mice (untreated). T cells from each of these groups were then transferred to naive recipient mice following implantation of MB49 bladder tumors (Fig. 4G). T cells from the MB49+BCG group, but not BCG only, were sufficient to confer resistance to bladder tumors in the absence of further BCG treatments (Fig. 4H). In contrast, transfer of polyclonal CD4 and CD8 T cells from mice that received only BCG into the bladders of naive mice did not confer any survival advantage as compared to transfer of T cells from PBS-treated mice (Fig. 4 I and J).

Taken together, these results demonstrate that BCG therapy for MB49 tumors induces CD4 T cell-dependent, tumor-specific immunity.

BCG Enhances Tumor-Specific T Cell Effector Function. Malignant transformation is accompanied by an accumulation of genetic mutations, a byproduct of which is the expression of aberrant proteins and peptides (termed neoantigens) that deviate enough in amino acid sequence to overcome self-tolerance to be recognized by the immune system. It is increasingly recognized that many tumors harbor tumor-infiltrating lymphocytes that are specific for tumor neoantigens (28). Moreover, activation of these tumor-specific tumor-infiltrating lymphocytes leading to tumor rejection or immuno-editing has been shown in the context of other immunotherapies, particularly checkpoint blockade therapy (21, 29, 30). The data presented above suggest that BCG could be driving a T cell response against neoantigens expressed by MB49 cells.

In order to study tumor-specific T cell responses, we developed a model of tumor neoantigens in which MB49 tumor cells express antigenic epitopes recognized by T cells from established TCR-transgenic mouse strains. We transduced MB49 cells with a plasmid encoding green fluorescent protein (GFP) fused to the ovalbumin epitopes recognized by TCR-transgenic OT-I CD8 T cells (SIINFEKL) and TCR-transgenic OT-II CD4 T cells (ISQAVHAAHAEINEAGR) (*SI Appendix*, Fig. S5A) (31, 32). We confirmed that MB49 tumors transduced with this plasmid (MB49^{OVA}) induce proliferation of adoptively transferred OT-I and OT-II T cells (*SI Appendix*, Fig. S5B). We confirmed that the majority of CD8 T cells from OT-I mice and CD4 T cells from OT-II mice have a naive phenotype at baseline (*SI Appendix*, Fig. S5C).

Next, we implanted MB49^{OVA} tumors into the bladders of mice and determined the effect of BCG on the phenotype and function of adoptively transferred CD4 and CD8 tumor-specific T cells within whole bladders and bladder-draining lymph nodes (Fig. 5). The absolute numbers of CD4 and CD8 T cells in the bladders and bladder-draining LNs did not differ between PBS- and BCG-treated mice (*SI Appendix*, Fig. S5D). Similarly, the overall abundance of OT-I and OT-II T cells in the bladder-draining LNs was similar in PBS- and BCG-treated mice (*SI Appendix*, Fig. S5E). Numbers of OT-I T cells in the bladders of BCG- and PBS-treated mice were similar, although there were fewer OT-II T cells in the bladders of BCG-treated animals than there were in PBS-treated animals (Fig. 5B).

BCG enhanced the activation and differentiation of tumor-specific CD4 and CD8 T cells, as measured by CD44 and CD62L expression (Fig. 5 C–E). In tumor-specific CD4 T cells, BCG also reduced T cell exhaustion, as measured by expression of PD-1 and LAG-3 (Fig. 5G). Moreover, tumor-specific CD4 T cells from the bladders of BCG-treated mice exhibited enhanced production of IFN-γ as compared to PBS-treated controls (Fig. 5I). In line with this finding, the endogenous repertoire of CD4 T cells, which presumably contains numerous tumor-specific T cell clones, also displayed enhanced production of IFN-γ, as well as TNF-α (*SI Appendix*, Fig. S5D).

Overall, these data indicate that BCG results in improved activation and reduced exhaustion of tumor-specific T cells, particularly tumor-specific CD4 T cells. These cells also exhibit enhanced production of IFN-γ, suggesting that BCG therapy results in enhanced tumor-specific T cell effector functions in the bladder tumor microenvironment.

BCG-Induced Antitumor Immunity Depends on Tumor-Intrinsic IFN-γ Signaling. The data described above demonstrate increased production of IFN-γ by tumor-specific CD4 T cells, and it was previously shown that IFN-γ knockout mice with bladder tumors do not respond to BCG (33). However, the cellular target of IFN-γ, whether tumor or immune cells, is not known. We initially explored the hypothesis that IFN-γ from tumor-specific T cells could signal directly to the tumor cell by assaying IFNGR expression and the response of MB49 cells to IFN-γ in vitro. We found that MB49 cells constitutively express IFNGR (Fig. 6A) and respond to IFN-γ by downregulating IFNGR and strongly up-regulating MHC class I and MHC class II, indicating a functional IFN-γ signaling pathway (Fig. 6 A and B).

To determine the role of IFN-γ signaling in bladder tumors, we generated an IFNGR knockout MB49 cell line using CRISPR gene editing (MB49^{IFNGRKO}) and confirmed that these cells no longer express IFNGR and no longer respond to IFN-γ in vitro (Fig. 6 A and B). The growth rate of MB49^{IFNGRKO} in vitro did not differ from wild-type MB49 (*SI Appendix*, Fig. S6). Next, we implanted mice with wild-type MB49 or MB49^{IFNGRKO} bladder tumors and found that the efficacy of BCG is completely abrogated in mice bearing MB49^{IFNGRKO} tumors (Fig. 6C). Moreover, mice with MB49^{IFNGRKO} fared even worse than PBS-treated control mice bearing wild-type MB49 tumors, providing additional evidence that, even in the absence of BCG treatment, immunosurveillance is occurring, albeit at a level insufficient to overcome the tumor.
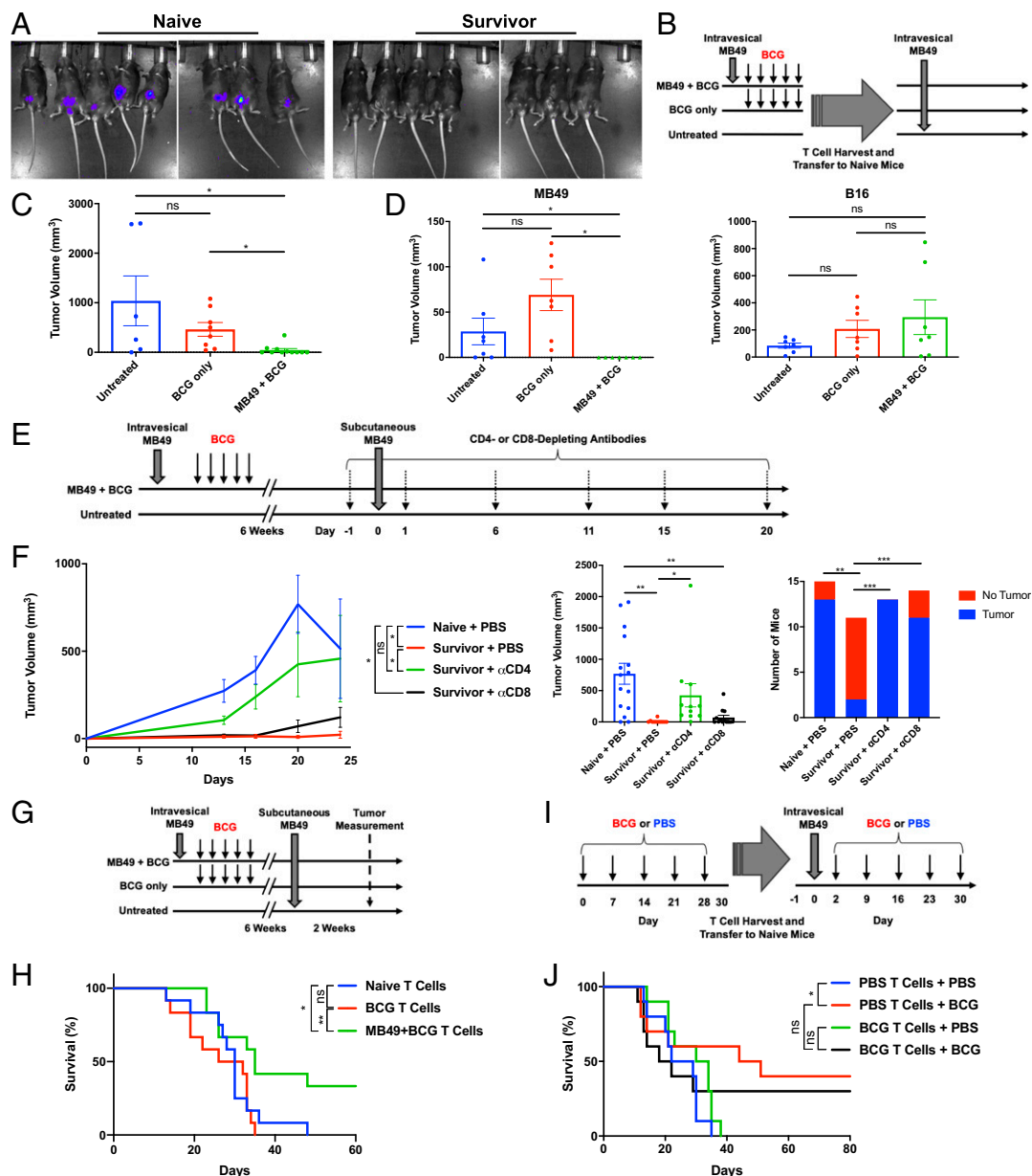
Antonelli et al.

Fig. 4. BCG stimulates long-term tumor-specific immunity. (*A*) Mice were implanted with MB49 bladder tumors and treated with BCG to generate a cohort of survivor mice. Six weeks after the final treatment, survivor mice or naive control mice were rechallenged with intravesical MB49 tumors expressing luciferase, and imaged 1 wk later to determine tumor rejection. (*B*) Experimental schematic. Mice were divided into three groups. Group 1 (MB49+BCG) were implanted with MB49 bladder tumors followed by five weekly intravesical BCG treatments. Group 2 (BCG only) received five weekly intravesical BCG treatments only. Group 3 (untreated) received neither MB49 nor BCG. Six weeks after the last treatment, 2×10^5 MB49 cells were injected subcutaneously in one flank. Tumor volume was measured 2 wk later. (*C*) Results of the experiment described in *B*. Data represent three independent experiments. *P* values were derived by one-way ANOVA with Bonferroni's multiple comparisons test. (*D*) Mice were divided into three groups as described in *B*. Six weeks after completion of the last treatment, 2×10^5 MB49 cells were injected subcutaneously in one flank and 2×10^5 B16 cells were injected subcutaneously in the opposite flank. Tumor volume was determined 2 wk later. Data are representative of two independent experiments. *P* values were derived by one-way ANOVA with Bonferroni's multiple comparisons test. (*E*) Experimental schematic. Mice were divided into two groups. Group 1 (MB49+BCG) were implanted with MB49 bladder tumors followed by five weekly intravesical treatments of BCG. Group 2 (untreated) received neither intravesical MB49 nor BCG. Six weeks after completion of the last treatment, 2×10^5 MB49 cells were injected subcutaneously in one flank. Mice received intraperitonel injections of anti-CD4 (αCD4) or anti-CD8 (αCD8) antibodies (or PBS) as shown. Tumor volumes were measured. (*F*) BCG-induced tumor-specific immunity is CD4-dependent. Results of the experiment described in *E*. Data are representative of two independent experiments. (*Left*) Tumor volume as function of time. (*Center*) Tumor volumes on day 20. *P* values were derived by one-way ANOVA with Bonferroni's multiple comparisons test. (*Right*) Proportion of tumor-bearing mice at day 20. *P* values were derived by Fisher's exact test. (*G*) Experimental schematic. Mice were divided into three groups as shown in *B*. Three days after completion of the last treatment, mice were killed and spleens were removed for T cell isolation; 2×10^6 T cells per mouse from each donor group were transferred to three groups of naive recipient mice. Intravesical MB49 tumors were instilled 1 d after T cell transfer. (*H*) Survival curves from *G*. Data are representative of two independent experiments. *P* values derived by log-rank test. (*I*) Experimental schematic. Tumor-free mice received weekly treatments of intravesical BCG or PBS; 6 wk after the last BCG treatment, spleens were removed and T cells were isolated. Naive recipient mice received 2×10^6 T cells per mouse via retro-orbital injection; 1 d after the T cell transfer, recipient mice were implanted with MB49 bladder tumors, followed by five weekly intravesical instillations of BCG or PBS beginning 2 d after tumor implantation. (*J*) Survival curves from *I*. Data represent two independent experiments. *P* values derived by log-rank test. Error bars in figure represent mean ± SD. See also *SI Appendix*, Fig. S3. *$P < 0.05$; **$P < 0.005$; ***$P < 0.0005$; ns, nonsignificant.

www.manaraa.com

Next, we determined the requirement for tumor cell IFNGR expression in long-term BCG-induced tumor-specific immunity. Survivor mice with BCG-induced tumor immunity and naive mice were challenged with subcutaneous wild-type MB49 or MB49^{IFNGRKO} tumors and tumor growth was measured over time (Fig. 6D). As expected, naive mice demonstrated growth of subcutaneous wild-type MB49 tumors, whereas survivor mice rejected wild-type MB49 tumors. In contrast, four of five survivor mice were unable to reject MB49^{IFNGRKO} tumors. Of note, naive mice bearing MB49^{IFNGRKO} tumors displayed more aggressive tumor growth than naive mice bearing wild-type tumors, again suggesting that tumor cell IFNGR signaling plays a role in immunosurveillance of MB49 tumors even in untreated mice.

To determine whether abrogation of the IFNGR-mediated response to BCG depends on expression of MHC class II on tumor cells, we generated an MHC class II knockout MB49 cell line using CRISPR gene editing (MB49^{MHCIIKO}). We confirmed that MB49^{MHCIIKO} cells did not express MHC class II at baseline nor in response to IFN-γ stimulation (Fig. 6E). However, despite loss of MHC class II expression, BCG remained effective in mice implanted with MB49^{MHCIIKO} tumors (Fig. 6F). Furthermore, MB49^{MHCIIKO} were efficiently rejected in survivor mice after establishment of BCG-induced MB49 tumor immunity (Fig. 6G).

These data demonstrate that tumor cell IFN-γ signaling is crucial to both the initial BCG-induced antitumor immune response and to subsequent tumor-specific CD4 T cell-mediated tumor rejection in a mechanism that is independent of tumor expression of MHC class II.

Discussion

Using the MB49 orthotopic model of bladder cancer, we found that bacterial immunotherapy for bladder cancer using BCG results in an enhanced tumor-specific T cell response, leading to T cell-dependent tumor-specific immunity. Although both CD4 and CD8 T cells are required for BCG-induced bladder tumor elimination, long-term tumor-specific immunity resulting from BCG therapy is predominantly CD4 T cell-dependent. Furthermore, our data demonstrate that one major effect of BCG is to enhance the effector functions of tumor-specific CD4 T cells, specifically IFN-γ production. Enhanced production of both IFN-γ and TNF-α was also observed in the endogenous CD4 T cell population of BCG-treated mice. This enhanced production of IFN-γ by BCG-treated tumor-specific T cells would be capable of signaling directly to the tumor cell via tumor-intrinsic IFNGR signaling, which we show is required for tumor elimination.

Although BCG resulted in the proliferation and expansion of BCG-specific T cells, attenuation of transport of BCG to the bladder-draining LNs did not affect BCG efficacy. These findings could suggest that BCG-specific T cell priming is not required for tumor elimination and that it may be sufficient for BCG to exert its effects locally on cell types within the bladder, although it is also possible that T cell priming occurs in tertiary lymphoid structures within the tumor, as has been observed in the context of checkpoint blockade therapy for melanoma (34), a scenario that requires further investigation. Moreover, transfer of BCG-specific T cells from P25 mice or from BCG-treated nontumor-bearing mice did not augment BCG efficacy. These findings are seemingly in contrast with the conclusions of Biot et al. (14), who inferred that BCG transport to the bladder-draining LNs and the subsequent recruitment of BCG-specific T cells to the bladder was required for the efficacy of BCG therapy. Although our data do not conclusively rule out a role for BCG-specific T cells in the antitumor effect of BCG, it is possible to reconcile the apparent contrast between our findings in a model where the crucial effect of BCG immunization is on innate immunity. Systemic immunization with BCG results in epigenetic changes in innate immune cells, such as monocytes, macrophages, and natural killer cells (35, 36), a process that has been suggested to occur in the context of BCG treatment for bladder cancer (37). In a model that reconciles our data with that of Biot et al. (14), activation of innate immune cells resulting from systemic immunization with BCG could lead to enhanced activation of tumor-specific T cells in the bladder.

Our data demonstrate that BCG leads to enhanced activation, reduced exhaustion, and ultimately enhanced effector function of tumor-specific T cells, with the most prominent phenotypes observed in the CD4 T cell compartment. In a recently published study, CD4 T cells that specifically recognized an MHC class II-restricted tumor neoantigen were identified in a patient with high-grade NMIBC (23), supporting our findings and providing the foundation for a mechanism in which BCG enhances the activity of previously dysfunctional tumor-specific T cells. The mechanism by which BCG leads to enhanced activation of tumor-specific T cells remains to be elucidated. Further studies are required to address the processes that occur upstream of T cell activation, which presumably involve a major role for antigen-presenting cells, and innate immune cells more generally.

Our findings that CD4 T cells play an especially critical role in the initial efficacy of BCG, as well as in the long-term tumor-specific immunity generated by BCG, is seemingly distinct from the cellular requirements of other immunotherapies for cancer. In the case of immune checkpoint blockade with PD-1 and programmed death-ligand 1 (PD-L1) antibodies, the most important immune cell subset appears to be CD8 T cells (19–22, 38), although there is an emerging appreciation for the role of CD4 T cells in this context as well (39). CD8 T cells also appear to be of critical importance in treatments using oncolytic viruses (40–42). These apparently divergent cellular requirements hint at distinct mechanisms of action for BCG therapy and suggest a potential advantage for strategies utilizing the immunological concepts inherent in BCG therapy for cases in which other immunotherapies have failed, or that using these concepts in combination with other immunotherapies could demonstrate a synergistic effect.

We found that expression of IFNGR on cancer cells was essential for the efficacy of BCG therapy, and our data suggest a compelling mechanism wherein IFN-γ secreted by tumor-specific T cells directly affects tumor cells through IFN-γ signaling, a hypothesis that is bolstered by studies showing that expression of IFNGR by cancer cells is important for the elimination phase of tumor immuno-editing (43, 44). Down-regulation of IFNGR expression by tumor cells is also a documented mechanism of immune escape, as in the context of treatment with PD-1–blocking antibodies, wherein IFNGR-induced PD-L1 expression by tumors is rendered ineffective as a means of inhibiting T cells, and selection subsequently shifts in favor of tumors with reduced responsiveness to IFN-γ as a means of reducing antigen presentation and other antiproliferative effects (45). In the context of BCG therapy, the mechanism by which tumor cell IFNGR expression affects the efficacy of treatment remains to be determined. One possibility is that IFN-γ enhances the immunogenicity of tumor cells by inducing expression of components of the antigen processing and presentation pathways (46); however, we found that expression of MHC class II on tumor cells was dispensable for treatment efficacy. Another is that IFN-γ acts by directly reducing tumor growth or inducing apoptosis (47–49), or possibly through enhanced responsiveness to TNF-α by tumor cells.

In summary, our data define the immunologic mechanism of antitumor immunity induced by the only Food and Drug Administration-approved bacterial therapy for cancer. These findings indicate that BCG enhances activation and IFN-γ production, as well as reduces exhaustion of tumor-specific T cells, leading ultimately to tumor-specific immunity. This tumor-specific
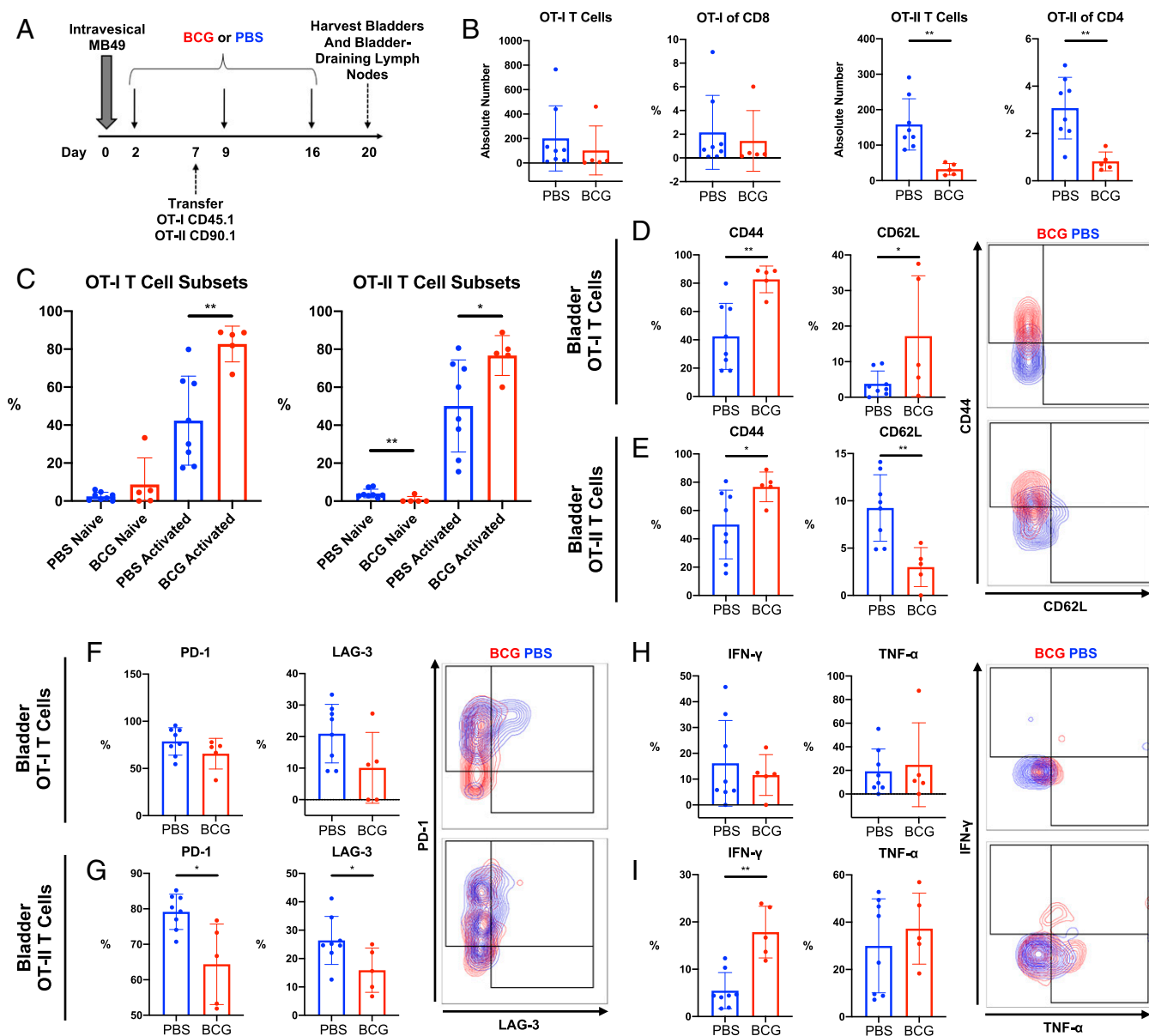
Fig. 5. BCG therapy results in enhanced tumor-specific T cell function. (*A*) Experimental schematic. Mice were implanted with MB49^{OVA} on day 0 followed by intravesical BCG or PBS on days 2 and 9. On day 7, 1 to 3 × 10^6 OT-I (CD45.1) and OT-II (CD90.1) T cells were transferred to recipient mice via retro-orbital injection. On day 20, whole bladders and bladder-draining lymph nodes were removed and analyzed by flow cytometry. (*B*–*I*) Comparison of BCG- versus PBS-treated bladders for the following: (*B*) Absolute numbers and percent OT-I and OT-II of total CD8 and CD4 T cells, respectively. (*C*) OT-I and OT-II T cell activation in the bladder, defined as naive (CD44$^-$CD62L$^+$) or activated (CD44$^+$). (*D* and *E*) Hallmark activation marker expression in OT-I or OT-II T cells, as measured by percent CD44$^+$ and CD62L$^+$. Representative flow plots are shown. (*F* and *G*) Hallmark exhaustion marker expression in OT-I or OT-II T cells, as measured by percent PD-1$^+$ and LAG-3$^+$. Representative flow plots are shown. (*H* and *I*) IFN-γ and TNF-α production by OT-I or OT-II T cells following ex vivo stimulation with PMA and ionomycin. Representative flow plots are shown. Error bars in figure represent mean ± SD. See also *SI Appendix*, Fig. S5. *$P < 0.05$; **$P < 0.005$; ns, nonsignificant.

immunity relies on a dynamic cross-talk between the immune system and tumor cells, mediated in part by a requirement for tumor cell IFN-γ signaling, through a complex mechanism that requires further investigation. These findings imply that BCG (the oldest immunotherapy for cancer) is similar to more recently employed checkpoint inhibitor strategies with regard to the induction of tumor-specific immunity and a requirement for tumor cell IFN-γ signaling, but also define some distinct features of the effect of BCG on tumor-specific CD4 T cells. Finally, these new immunologic insights may allow investigation into biomarkers that could predict the efficacy of BCG in human cancer patients.

Materials and Methods

Cell Lines. The mouse bladder cancer cell line MB49, expressing luciferase under G418 selection, was a gift from Yi Luo, University of Iowa, Iowa City, IA. All experiments performed throughout this report utilized luciferase-expressing MB49 cell lines. The mouse melanoma cell line B16 was obtained from Taha Merghoub, Memorial Sloan Kettering Cancer Center, New York, NY. MB49 and B16 were grown in RPMI supplemented with 10% FBS, and 2 mM L-glutamine. For MB49, G418 (Sigma) was added at a concentration of 800 μg/mL to select for luciferase-expressing cells. Cells were cultured at 37 °C in a humidified atmosphere of 5% CO$_2$. All cell lines used were confirmed to be negative for mycoplasma by annual testing using MycoAlertTMPlus (Lonza). Last testing was performed on 14 August 2019.
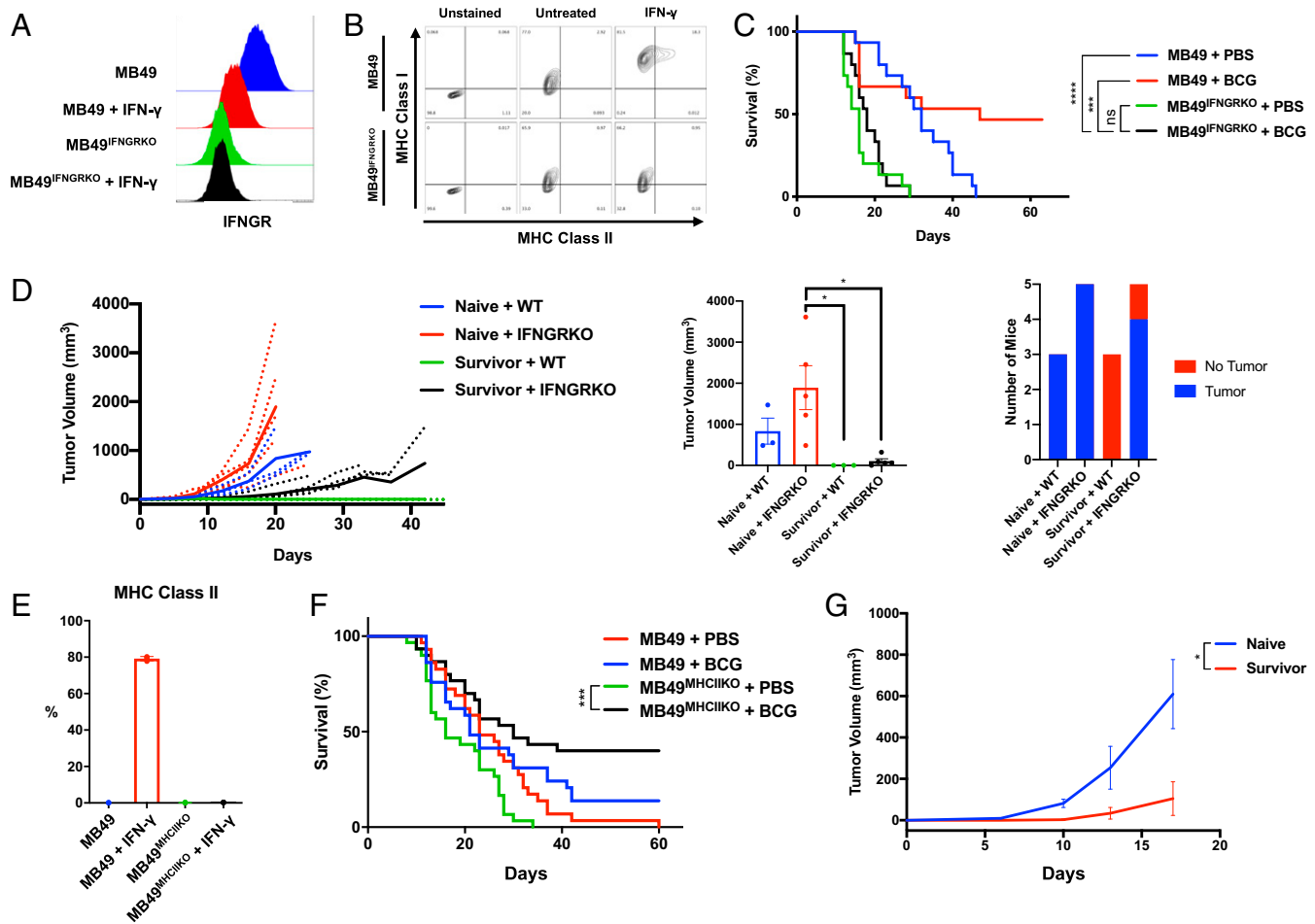
www.manaraa.com

Fig. 6. BCG-induced tumor elimination requires expression of IFNGR on tumor cells. (*A*) Histograms of baseline IFNGR expression by wild-type MB49 and MB49[IFNGRKO], with or without IFN-γ stimulation, as measured by flow cytometry. (*B*) Expression of MHC class I (*y* axis) and MHC class II (*x* axis) in wild-type MB49 and in MB49[IFNGRKO], with or without IFN-γ stimulation. (*C*) Survival curves of mice implanted with wild-type MB49 or MB49[IFNGRKO] tumors. Mice were treated with BCG or PBS on days 2, 9, 16, 23, and 30 after tumor implantation. *P* values derived by log-rank test. (*D*) Survivor mice were generated by implantation of MB49 bladder tumors followed by five weekly intravesical treatments of BCG. Six weeks after completion of the last BCG treatment, 2×10^5 wild-type MB49 or MB49[IFNGRKO] cells were injected subcutaneously into the flanks of survivor mice and age-matched naive mice. Tumor volume was determined at the specified time points. (*Left*) Tumor volume as a function of time. (*Center*) Tumor volumes on day 20. Error bars represent mean ± SD. *P* values were derived by one-way ANOVA with Bonferroni's multiple comparisons test. (*Right*) Proportion of tumor-bearing mice at day 20. (*E*) Percent of cells expressing MHC class II as determined by flow cytometry in wild-type MB49 and in MB49[MHCIIKO], with or without IFN-γ stimulation. (*F*) Survival curves of mice implanted with wild-type MB49 or MB49[MHCIIKO] tumors. Mice were treated with BCG or PBS on days 2, 9, 16, 23, and 30 after tumor implantation. *P* values derived by log-rank test. (*G*) Survivor mice were generated by implantation of MB49 bladder tumors followed by five weekly intravesical treatments of BCG. Six weeks after completion of the last BCG treatment, 2×10^5 wild-type MB49 or MB49[MHCIIKO] cells were injected subcutaneously into the flanks of survivor mice and age-matched naive mice. Tumor volume was determined at the specified time points. See also *SI Appendix*, Fig. S6. *$P < 0.05$; ***$P < 0.0005$; ns, nonsignificant.

BCG. The *Pasteur* strain of BCG was grown at 37 °C in Middlebrook 7H9 supplemented with 10% albumin/dextrose/saline, 0.5% glycerol, and 0.05% Tween 80. To create titered stocks for infection, BCG was grown to midlog phase (OD_{600} 0.4 to 0.6), washed twice in PBS with 0.05% Tween 80, resuspended in PBS with 25% glycerol, and stored at −80 °C. To measure the final bacterial titer, an aliquot was thawed and serial dilutions were cultured on 7H10 agar. The bacterial titer was then determined by counting colonies after 3 wk of incubation.

Mouse Strains. C57BL/6 (stock #000664), OT-I (stock #003831), OT-II (stock #004194), P25 (stock #011005), CD45.1 (stock #002014), and CD90.1 (stock #000406) mice were purchased from The Jackson Laboratory. C7 mice were generated by our laboratory, as previously described (27). CCR2-DTR mice were generated as previously described (50). OT-I and OT-II mice were crossbred with CD45.1 and CD90.1 mice, respectively. P25 mice were crossbred with CD45.1 mice. All mouse strains were bred and housed in Memorial Sloan Kettering Cancer Center's (MSKCC) Research Animal Resource Center under specific pathogen-free conditions. To deplete inflammatory monocytes, CCR2-DTR mice or their cohoused control littermates were injected

intraperitoneally with 200 ng (10 ng/g body weight) of DT (List Biological Laboratories) as noted for a total of four doses.

All animal studies were performed with approval from the MSKCC Institutional Animal Care and Use Committee under Protocol 01-11-030 and were compliant with all applicable provisions established by the Animal Welfare Act and the Public Health Services Policy on the Humane Care and Use of Laboratory Animals.

MB49 Orthotopic Implantation. The MB49 orthotopic bladder cancer model is outlined in *SI Appendix*, Fig. S1A. Six- to 8-wk-old female mice (The Jackson Laboratory) were placed under anesthesia in an isoflurane chamber. A 24-gauge catheter (Terumo) was inserted into the bladder through the urethra. Next, 100 μL of poly-L-lysine (Sigma) was injected through the catheter, the catheter was capped using an injection plug (Terumo), and the mice were kept under anesthesia for 30 min. The catheter was then removed and flushed with a solution containing 500,000 MB49 cells/mL in RPMI. The mouse was removed from the isoflurane chamber, the bladder was manually emptied, and the catheter was reinserted. Nextm 100 μL of the MB49 solution (~50,000 cells per mouse) was injected into the bladder and the catheter

was recapped. The mice were kept under anesthesia for 1 h. At the end of the hour, catheters were removed, and the mice were allowed to recover from anesthesia.

One week after MB49 implantation, mice were injected with D-luciferin potassium salt (GoldBio) and imaged using an IVIS spectrum in vivo imaging system to confirm uptake of tumor cells in the bladder. In all experiments we had tumor uptake rates of 93 to 100%. Mice that did not exhibit tumor uptake at the 1-wk timepoint were excluded from analysis. Mice were observed daily and were killed if they displayed signs of distress, such as dull fur, apathy, or visible signs of growing tumor.

Intravesical BCG Treatment. Frozen titered stocks of BCG (prepared as detailed above) were thawed and resuspended in PBS for a final concentration of 3×10^7 colony forming units/mL (CFU/mL). PBS alone was used as control. For intravesical treatment, mice were placed under anesthesia in an isoflurane chamber. A 24-gauge catheter (Terumo) was inserted into the bladder through the urethra, and 100 μL of BCG ($\sim 3 \times 10^6$ CFU per mouse) or PBS was injected into the bladder. The catheter was capped using an injection plug (Terumo). The mice were kept under anesthesia for 2 h. At the end of this time, catheters were removed and the mice were allowed to recover from anesthesia.

Measurement of Subcutaneous Tumors. The size of subcutaneous tumors was determined by caliper measurement. Tumor volume was estimated using the formula (tumor volume) = [(tumor width)^2 × (tumor length)]/2.

Preparation of Bladder Single-Cell Suspensions. Tumor-bearing mice were killed and bladders were harvested. Bladders were minced and transferred to a tube containing 1 mg/mL collagenase type I (Invitrogen) and 2 KU/mL of DNase I, type IV (Sigma) in serum-free RPMI. Tubes were incubated at 37 °C on a rotating apparatus for 1 h. Suspensions were passed through a 70-μm filter (Invitrogen). Lysis of red blood cells (RBCs) was performed using RBC Lysis Buffer (Invitrogen).

Flow Cytometry. Cell suspensions were analyzed on an LSR II or Fortessa flow cytometer (BD Biosciences), using FACS DiVa software (BD Biosciences) according to the manufacturer's instructions. Data analysis was performed using the FlowJo software package (Tree Star).

MB49 bladder tumor size and composition are heterogeneous both within and between groups. Bladder tumors grow diffusely throughout the entirety of the bladder epithelium, rendering healthy and tumor tissue virtually indistinguishable, and due to the fact that the bladder lumen often contains necrotic debris that is difficult to separate from viable tumor tissue, we have found that bladder weights do not accurately reflect the size of tumors nor serve as a reliable denominator for calculating absolute numbers of cells per tumor weight. We show absolute numbers of cells as the number of cells in the entirety of a bladder sample, run through the flow cytometer to completion, in addition to showing the percentages of cells in each sample.

For determination of cytokine production by T cells, single-cell suspensions were enriched for immune cell infiltrates using Percoll (GE Healthcare) gradient centrifugation. The immune cells were restimulated with 500 ng/mL PMA and 1 mg/mL ionomycin and incubated for 4 h at 37 °C in the presence of Brefeldin A. Staining with antibodies against extracellular antigens was performed first. The stained cells were then fixed and permeabilized using Foxp3 Fixation/Permeabilization Buffer (eBioscience) according to the manufacturer's instructions, followed by staining for intracellular antigens. Antibodies used for this study are detailed in *SI Appendix*, Table S1.

CD4 and CD8 T Cell Depletion. Mice were injected intraperitoneally with two initial doses of 500 μg of anti-CD4 (*InVivo*Plus Clone GK1.5, BioXCell #:

BP0003-1) or anti-CD8 antibodies (*InVivo*Plus Clone 2.43, BioXCell #: BP0061) 2 d apart followed by 250 μg of anti-CD4 or anti-CD8 antibodies every 5 d until the end of the experiment. Depletion efficiency was determined by flow cytometric analysis of PBMCs obtained 7 d after initiation of depletion.

Cell Isolation and Adoptive Transfer. Spleens were removed, and single-cell suspensions were made. CD4$^+$ and CD8$^+$ cells were isolated using a mouse CD4$^+$ T Cell Isolation Kit and CD8$^+$ T Cell Isolation Kit, respectively (Miltenyi). Total T cells were isolated using a mouse Pan T Cell Isolation Kit II (Miltenyi). Cells were counted and resuspended in serum-free media. Mice were placed under anesthesia in an isoflurane chamber and the cells were transferred via retro-orbital injection. For proliferation experiments, T cells were incubated with CellTrace Violet proliferation dye (ThermoFisher) prior to adoptive transfer, according to the manufacturer's protocol. Proliferation was measured by CellTrace Violet dilution at the specified timepoint using flow cytometry.

Generation of IFNGR and MHCII Knockout MB49 Cell Lines. MB49^{IFNGRKO} and MB49^{MHCIIKO} were generated with help from the Gene Editing and Screening Core at MSKCC. For each gene, three candidate plasmid constructs were designed using the transient plasmid PX458 [pSpCas9(BB)-2A-GFP; Addgene, Plasmid #48138]. Each candidate plasmid contained a GFP reporter, CRISPR/Cas9, and single guide RNA specific to a region of the IFNGR1 gene or H2-Ab1 gene, selected to minimize off-target effects. Our parental MB49 cell line expressing luciferase under G418 selection was transfected with each of the candidate plasmids using Lipofectamine 2000 (Invitrogen) according to the manufacturer's protocol. These transformed cell line candidates were sorted for purity (based on GFP positivity and IFNGR negativity for the IFNGR knockout or GFP positivity and MHC class II negativity for the MHC class II knockout). The final cell line used for IFNGR knockout experiments utilized the gRNA sequence CGACTTCAGGGTGAAATACG, which targeted the IFNGR1 gene at codons 19603812 to 19603834, and was selected based on functional testing, including IFNGR negativity and no up-regulation of MHC class I or class II following stimulation with recombinant mouse IFN-γ (Fisher) at a concentration of 100 ng/mL for 48 h. The final cell line used for MHC class II knockout experiments utilized the gRNA sequence GTAGACCTCTCC CCGCCGAG, which targeted the H2-Ab1 gene at codons 34267543 to 34267565 and was selected based on functional testing (no expression of MHC class II at baseline nor following IFN-γ stimulation as detailed above).

Statistical Analysis. The group means for different treatments were compared, as indicated, by ANOVA with Bonferroni's multiple comparisons test, or by a two-sided Student's *t* test. Fisher's exact test was used for analysis of categorical values. For survival analyses, groups were compared by log-rank (Mantel–Cox) test. P values ≤ 0.05 were considered significant.

Data Availability. All data are included in the main text or *SI Appendix*.

1. W. B. Coley, The treatment of malignant tumors by repeated inoculations of erysipelas. With a report of ten original cases. 1893. *Clin. Orthop. Relat. Res.*, 3–11 (1991).
2. W. B. Coley, The treatment of inoperable sarcoma by bacterial toxins (the mixed toxins of the Streptococcus erysipelas and the Bacillus prodigiosus). *Proc. R. Soc. Med.* **3**, 1–48 (1910).
3. L. J. Old, D. A. Clarke, B. Benacerraf, Effect of Bacillus Calmette-Guerin infection on transplanted tumours in the mouse. *Nature* **184** (suppl. 5), 291–292 (1959).
4. G. Mathé et al., Active immunotherapy for acute lymphoblastic leukaemia. *Lancet* **1**, 697–699 (1969).
5. D. L. Morton et al., BCG immunotherapy of malignant melanoma: Summary of a seven-year experience. *Ann. Surg.* **180**, 635–643 (1974).
6. A. Morales, D. Eidinger, A. W. Bruce, Intracavitary Bacillus Calmette-Guerin in the treatment of superficial bladder tumors. *J. Urol.* **116**, 180–183 (1976).
7. R. F. Han, J. G. Pan, Can intravesical bacillus Calmette-Guérin reduce recurrence in patients with superficial bladder cancer? A meta-analysis of randomized trials. *Urology* **67**, 1216–1223 (2006).
8. M. D. Shelley et al., A systematic review of intravesical bacillus Calmette-Guérin plus transurethral resection vs transurethral resection alone in Ta and T1 bladder cancer. *BJU Int.* **88**, 209–216 (2001).
9. R. J. Sylvester, A. P. van der MEIJDEN, D. L. Lamm, Intravesical bacillus Calmette-Guerin reduces the risk of progression in patients with superficial bladder cancer: A meta-analysis of the published results of randomized clinical trials. *J. Urol.* **168**, 1964–1970 (2002).
10. N. S. Forbes et al., White paper on microbial anti-cancer therapy and prevention. *J. Immunother. Cancer* **6**, 78 (2018).
11. G. Redelman-Sidi, M. S. Glickman, B. H. Bochner, The mechanism of action of BCG therapy for bladder cancer—A current perspective. *Nat. Rev. Urol.* **11**, 153–162 (2014).
12. T. L. Ratliff, J. K. Ritchey, J. J. Yuan, G. L. Andriole, W. J. Catalona, T-cell subsets required for intravesical BCG immunotherapy for bladder cancer. *J. Urol.* **150**, 1018–1023 (1993).
13. C. Pettenati, M. A. Ingersoll, Mechanisms of BCG immunotherapy and its outlook for bladder cancer. *Nat. Rev. Urol.* **15**, 615–625 (2018).

14. C. Biot et al., Preexisting BCG-specific T cells improve intravesical immunotherapy for bladder cancer. Sci. Transl. Med. 4, 137ra72 (2012).

15. W. Krajewski et al., Does Mantoux test result predicts BCG immunotherapy efficiency and severe toxicity in non-muscle invasive bladder cancer. Urol. J. 16, 458–462 (2019).

16. C. Y. Bilen, K. Inci, I. Erkan, H. Ozen, The predictive value of purified protein derivative results on complications and prognosis in patients with bladder cancer treated with bacillus Calmette-Guerin. J. Urol. 169, 1702–1705 (2003).

17. R. S. Svatek, C. Tangen, S. Delacroix, W. Lowrance, S. P. Lerner, Background and update for S1602 "A phase III randomized trial to evaluate the influence of BCG strain differences and T cell priming with intradermal BCG before intravesical therapy for BCG-naïve high-grade non-muscle-invasive bladder cancer.". Eur. Urol. Focus 4, 522–524 (2018).

18. T. K. Kopp, J. Batista da Costa, M. Mannas, P. C. Black, Current clinical trials in non-muscle invasive bladder cancer. Curr. Urol. Rep. 19, 101 (2018).

19. N. McGranahan et al., Clonal neoantigens elicit T cell immunoreactivity and sensitivity to immune checkpoint blockade. Science 351, 1463–1469 (2016).

20. M. Fehlings et al., Late-differentiated effector neoantigen-specific CD8+ T cells are enriched in peripheral blood of non-small cell lung carcinoma patients responding to atezolizumab treatment. J. Immunother. Cancer 7, 249 (2019).

21. M. Fehlings et al., Checkpoint blockade immunotherapy reshapes the high-dimensional phenotypic heterogeneity of murine intratumoural neoantigen-specific CD8+ T cells. Nat. Commun. 8, 562 (2017).

22. M. M. Gubin et al., Checkpoint blockade cancer immunotherapy targets tumour-specific mutant antigens. Nature 515, 577–581 (2014).

23. V. Leko et al., Identification of neoantigen-reactive tumor-infiltrating lymphocytes in primary bladder cancer. J. Immunol. 202, 3458–3467 (2019).

24. M. Kates et al., Intravesical BCG induces CD4+ T-cell expansion in an immune competent model of bladder cancer. Cancer Immunol. Res. 5, 594–603 (2017).

25. M. Samstein et al., Essential yet limited role for CCR2+ inflammatory monocytes during Mycobacterium tuberculosis-specific T cell priming. eLife 2, e01086 (2013).

26. T. Tamura et al., The role of antigenic peptide in CD4+ T helper phenotype development in a T cell receptor transgenic model. Int. Immunol. 16, 1691–1699 (2004).

27. A. M. Gallegos, E. G. Pamer, M. S. Glickman, Delayed protection by ESAT-6-specific effector CD4+ T cells after airborne M. tuberculosis infection. J. Exp. Med. 205, 2359–2368 (2008).

28. T. N. Schumacher, W. Scheper, P. Kvistborg, Cancer neoantigens. Annu. Rev. Immunol. 37, 173–200 (2019).

29. N. Riaz et al., Tumor and microenvironment evolution during immunotherapy with Nivolumab. Cell 171, 934–949.e16 (2017).

30. V. Anagnostou et al., Evolution of neoantigen landscape during immune checkpoint blockade in non-small cell lung cancer. Cancer Discov. 7, 264–276 (2017).

31. K. A. Hogquist et al., T cell receptor antagonist peptides induce positive selection. Cell 76, 17–27 (1994).

32. M. J. Barnden, J. Allison, W. R. Heath, F. R. Carbone, Defective TCR expression in transgenic mice constructed using cDNA-based alpha- and beta-chain genes under the control of heterologous regulatory elements. Immunol. Cell Biol. 76, 34–40 (1998).

33. J. Riemensberger, A. Böhle, S. Brandau, IFN-gamma and IL-12 but not IL-10 are required for local tumour surveillance in a syngeneic model of orthotopic bladder cancer. Clin. Exp. Immunol. 127, 20–26 (2002).

34. R. Cabrita et al., Tertiary lymphoid structures improve immunotherapy and survival in melanoma. Nature 577, 561–565 (2020).

35. E. Kaufmann et al., BCG educates hematopoietic stem cells to generate protective innate immunity against tuberculosis. Cell 172, 176–190.e19 (2018).

36. R. J. W. Arts et al., BCG vaccination protects against experimental viral infection in humans through the induction of cytokines associated with trained immunity. Cell Host Microbe 23, 89–100.e5 (2018).

37. K. Buffen et al., Autophagy controls BCG-induced trained immunity and the response to intravesical BCG therapy for bladder cancer. PLoS Pathog. 10, e1004485 (2014).

38. S. C. Wei et al., Distinct cellular mechanisms underlie anti-CTLA-4 and anti-PD-1 checkpoint blockade. Cell 170, 1120–1133.e17 (2017).

39. E. Alspach et al., MHC-II neoantigens shape tumour immunity and response to immunotherapy. Nature 574, 696–701 (2019).

40. P. K. Bommareddy, S. Aspromonte, A. Zloza, S. D. Rabkin, H. L. Kaufman, MEK inhibition enhances oncolytic virus immunotherapy through increased tumor cell killing and T cell activation. Sci. Transl. Med. 10, eaau0417 (2018).

41. C. J. LaRocca, S. G. Warner, Oncolytic viruses and checkpoint inhibitors: Combination therapy in clinical trials. Clin. Transl. Med. 7, 35 (2018).

42. A. Ribas et al., Oncolytic virotherapy promotes intratumoral T cell infiltration and improves anti-PD-1 immunotherapy. Cell 170, 1109–1119.e10 (2017).

43. D. H. Kaplan et al., Demonstration of an interferon gamma-dependent tumor surveillance system in immunocompetent mice. Proc. Natl. Acad. Sci. U.S.A. 95, 7556–7561 (1998).

44. A. S. Dighe, E. Richards, L. J. Old, R. D. Schreiber, Enhanced in vivo growth and resistance to rejection of tumor cells expressing dominant negative IFN gamma receptors. Immunity 1, 447–456 (1994).

45. J. M. Zaretsky et al., Mutations associated with acquired resistance to PD-1 blockade in melanoma. N. Engl. J. Med. 375, 819–829 (2016).

46. V. Shankaran et al., IFNgamma and lymphocytes prevent primary tumour development and shape tumour immunogenicity. Nature 410, 1107–1111 (2001).

47. L. Wall, F. Burke, C. Barton, J. Smyth, F. Balkwill, IFN-gamma induces apoptosis in ovarian cancer cells in vivo and in vitro. Clin. Cancer Res. 9, 2487–2496 (2003).

48. K. M. Detjen, K. Farwig, M. Welzel, B. Wiedenmann, S. Rosewicz, Interferon gamma inhibits growth of human pancreatic carcinoma cells via caspase-1 dependent induction of apoptosis. Gut 49, 251–262 (2001).

49. E. Alspach, D. M. Lussier, R. D. Schreiber, Interferon γ and its important roles in promoting and inhibiting spontaneous and therapeutic cancer immunity. Cold Spring Harb. Perspect. Biol. 11, a028480 (2019).

50. T. M. Hohl et al., Inflammatory monocytes facilitate adaptive CD4 T cell responses during respiratory fungal infection. Cell Host Microbe 6, 470–481 (2009).

IMMUNOLOGY AND INFLAMMATION

Antonelli et al.

www.manaraa.com